Electronic states in Cu_2MnX (X = Al, In, and Sn) Heusler alloy studied by XMCD and multiple scattering calculations

Shigeaki Uemura,[a*] Hiroshi Maruyama,[a] Naomi Kawamura,[b] Hitoshi Yamazaki,[a] Shin-ichi Nagamatsu[c] and Takashi Fujikawa[c]

[a]Department of Physics, Faculty of Science, Okayama University 3-1-1 Tsushima-Naka, Okayama, Okayama 700-8530, Japan, [b]Institute of Physics and Chemical Researches / SPring-8, 1-1-1 Kouto, Mikazuki, Sayo, Hyogo 798-5148, Japan, [c]Graduate School for Science, Chiba University 1-33 yayoi, Inage, Chiba, Chiba 263-0022, Japan.
Email: uemura@mag.okayama-u.ac.jp

X-ray magnetic circular dichroism (XMCD) has been measured at Mn and Cu *K*-edge in Cu_2MnX (X=Al, In, and Sn) Heusler alloy. The Mn *K*-edge spectrum shows a dispersion-type profile and the Cu *K*-edge resembles the Mn spectrum, which suggests that polarization of the *p* unoccupied bands originates commonly in Mn 3*d* states. To reproduce the observed spectrum by full multiple scattering calculations, Madelung potential has been taken into account. Charge redistribution is an important factor for the electronic structure in Cu_2MnX Heusler alloy.

Keywords : X-ray magnetic circular dichroism, *K*-absorption edge, photoelectron full multiple scattering calculation, Mn-Heusler alloy

1. Introduction

Cu_2MnX (X=Al, In, and Sn) Heusler alloy has the $L2_1$-type ordered structure consisting of eight bcc octants, in which Cu atoms form the octant and the body center is alternately occupied by Mn and X atoms. These alloys are ferromagnetic in spite of relatively large Mn-Mn inter-atomic distance with nonmagnetic elements. Neutron magnetic scattering has shown that Mn atom is responsible for the magnetic moments in these compounds and Cu atom also carries only $0.1\mu_B$ (Felcher *et al.*, 1963). The magnetic ordering has been interpreted due to the RKKY interaction between Mn 3*d* localized moments through *s, p* conduction electrons. The magnetic properties have been discussed in terms of magnetism associated with itinerant electrons (Shinohara, 1969). There is, however, few amount of research about magnetic polarization in the *s, p* conduction electrons, closely correlated with the 3*d* localized moments in a local environment, and about role of the conduction electrons for the magnetic ordering. To study electronic and magnetic states of the conduction electrons, X-ray magnetic circular dichroism (XMCD) at *K*-absorption edge is suitable, because the *K*-edge XMCD resulting from the $1s \rightarrow 4p$ transitions is very sensitive to the *p* unoccupied bands strongly hybridized with the 3*d* states. However, the spectrum is generally very weak and shows a complicated profile, so that precise spectrum and systematic simulations are highly desired for a better understanding.

2. Experimental

Samples prepared for this study were Cu_2MnX (X=Al, In, and Sn) Heusler alloys. The ingots were made from high purity Cu, Mn, Al, In, and Sn using arc furnace (X=Al) or induction furnace (X=In and Sn) in an Ar-gas atmosphere. Then, they were annealed for 24 hours at 800°C (X=Al) (Dunlap, R.A. 1986), 640°C (X=In), 580°C (X=Sn) and quenched into water for forming the $L2_1$-type superstructure. To verify the superstructure and to check single phase, X-ray diffraction measurements were carried out. Magnetic properties were also confirmed by magnetization measurements using SQUID. These powdered samples (<25μm) were uniformly spread out on the Scotch tape for X-ray absorption measurements.

XMCD spectrum was recorded in transmission mode at both the Mn and Cu *K*-edges using the left-circularly polarized X-rays (+ helicity) on BL-28B, KEK Photon Factory. (Iwazumi, 1989) X-ray intensity was monitored using ionization chambers before and after the sample: I_0 is the intensity of incident beam and I is that of transmitted beam. Magnetic field of 0.6 T was applied antiparallel or parallel to the direction of wave vector of the incident beam. Degree of circular polarization P_C was estimated to be 0.35 ~ 0.6 in the energy range measured. Absorption coefficient was recorded in an interval of 1 eV, and data were accumulated every 2 seconds, while the magnetic field was reversed twice for each point. XANES and XMCD spectra are defined as follows:

$$\text{(XANES)} \quad \mu t = (1/2)(\ln[I_0/I(\uparrow)] + \ln[I_0/I(\downarrow)]) \qquad (1)$$

$$\text{(XMCD)} \quad \Delta\mu t = \ln[I_0/I(\uparrow)] - \ln[I_0/I(\downarrow)], \qquad (2)$$

where $I(\uparrow)$ ($I(\downarrow)$) represents the intensity of transmitted X-ray with magnetization antiparallel (parallel) to the X-ray wave vector. Absorption edge energy E_0 was determined as the first inflection point of XANES spectrum. The XANES spectrum was normalized to unity by the edge-jump and XMCD spectrum was also subjected to the normalization and corrections.

3. Simulation

We simulated the XANES and XMCD spectra on the basis of photoelectron full multiple scattering (FMS) theory (Fujikawa 1993). The FMS offers a useful way for XANES theoretical calculation taking into account full multiple scattering. Moreover, polarization dependence, spin-orbit interaction and exchange scattering are also included in the FMS formalism. In this work, we used non-local exchange potential that can directly take the spin-polarization effects into account; however, correlation-potential was not included. Other potential dependence on spin polarization is also discussed (Hatada *et al*,. 2000). In the FMS simulations for 3*d* transition metal element, the spin-orbit interaction and the exchange scattering are main factors. The former operates photoelectrons ejected from the absorbing atom; the latter affects the scattering process. Thus, we have taken these effects into account for the present calculations of the *K*-edge XMCD.

The procedure for the XANES and XMCD calculation is as follows:

(1) Madelung potential

From the band calculation for Cu_2MnAl (Ishida *et al*,. 1978), electron population of several atomic orbitals and charge transfer between *p* and *d* states or *d* and *d* states were evaluated, and then Madelung potential was calculated on the muffin-tin approximation.

(2) Phase shift

To calculate phase shift, the following parameters were used: lattice constant, Madelung potential, muffin-tin radius, cluster size (up to the forth shell including 51 atoms), Z+1 approximation, and damping factor. In addition to these factors,

exchange potential was derived from the atomic wave function (Harman & Skilman, 1963) on the muffin-tin approximation.
(3) Full multiple scattering calculations

XANES spectrum was calculated using the phase shift calculated for each constituent atom. This procedure was iterated as far as the calculated spectrum was comparable with the experimental data. XMCD simulation was made following the XANES fitting procedure. The XMCD spectrum was simulated as a function of magnitude of spin polarization.

4. Experimental Results and Discussion

4.1 XANES and XMCD spectra

Figure 1 shows XANES and XMCD spectra at the *K*-edge of Mn and Cu in Cu_2MnX (X=Al, In, and Sn). The XANES profile resembles among them because of the isomorphic intermetallics. Some minor difference in the profile may come from modification in the electronic structure due to the third constituent element.

The XANES spectrum at the Mn *K*-edge commonly shows a crest that characterizes a bcc-like environment around Mn atom. Second and third oscillatory peaks indicate difference in the Mn-Mn interatomic distance due to lattice constant, Cu_2MnAl (a=5.95Å), Cu_2MnIn (6.19Å), and Cu_2MnSn (6.17Å). This may be associated with the difference in principal quantum number, 3*p* and 5*p*, of the most outer-shell electrons. This is related to the fact that the Cu *K*-edge XANES shows a fcc-like structure in Cu_2MnAl whereas Cu_2MnIn and Cu_2MnSn show a bcc-like profile. These XANES spectra show no pre-edge shoulder, which indicates the metallic nature in these materials. In particular, this trend is remarkable at the Cu *K*-edge.

The XMCD spectrum at the Mn *K*-edge shows a dispersion-type profile (Cu_2MnAl) or a negative single peak (Cu_2MnIn and Cu_2MnSn) around the edge. In Cu_2MnAl, the profile is asymmetric and relatively wide. The positive peak collapses in Cu_2MnIn and Cu_2MnSn, although the negative peak shows almost the same intensity as Cu_2MnAl has. This may be also associated with the difference between 3*p* and 5*p* electrons, because the 5*p* orbitals could be closely mixed with 4*p* electrons. Furthermore, additional dichroic spectrum recorded at $(E\text{-}E_0)\approx 50$ eV is identified as multi-electron excitation (MEE) (Kawamura, *et al*. 1999). Such a prominent MEE dichroic signal is the first observation in metallic compounds.

We have observed for the first time that the Cu *K*-edge yields a very sharp XMCD spectrum. It should be noted that Cu atom is also polarized magnetically in the Cu_2MnX Heusler alloy. In Cu_2MnAl, the XMCD shows an asymmetric and sharp profile, whereas in Cu_2MnIn and Cu_2MnSn the positive peak at just the edge disappeared, which corresponds to the observation at the Mn *K*-edge. What is the reason why the Cu *K*-edge XMCD is similar to that at the Mn *K*-edge? It may be commonly due to the polarization of Mn 3*d* states, which results in the polarization of *p*-conduction bands through the Mn 3*d*-4*p* intra-atomic interaction. Hence, the variation with the third constituent (X=Al, In, and Sn) is ascribed to the different contribution between 3*p* (Al: $3s^2 3p$) and 5*p* orbitals (In: $5s^2 5p$ and Sn: $5s^2 5p^2$) to both the Mn and Cu *K*-edge. Therefore, we speculate that the difference in wave function between 3*p* and 5*p* orbitals is an important factor.

4.2 Simulations

We have carried out the FMS calculations based on the semi-relativistic framework and compared with the experimental spectrum at the Mn and Cu *K*-edges. Figure 2 shows the

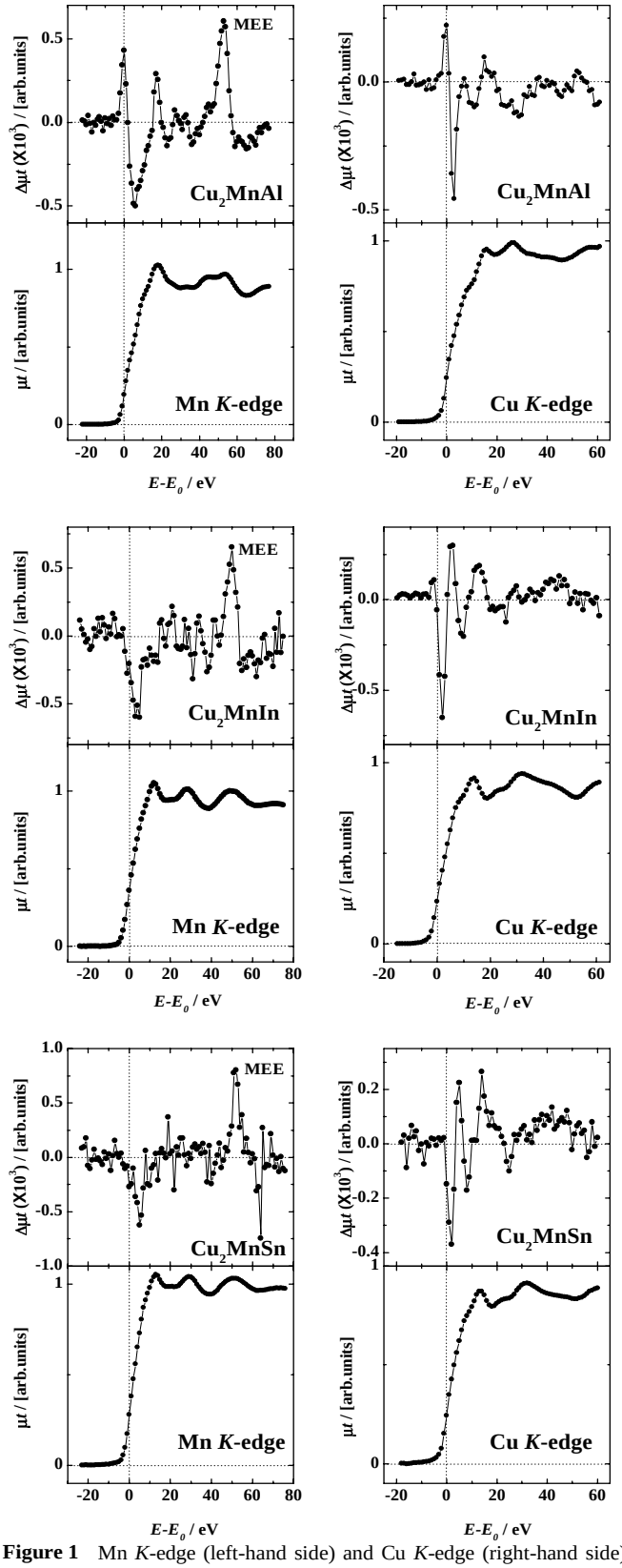

Figure 1 Mn *K*-edge (left-hand side) and Cu *K*-edge (right-hand side) in Cu_2MnX (X=Al, In, and Sn) alloy. The XMCD (XANES) spectrum is shown in upper (lower) panel.

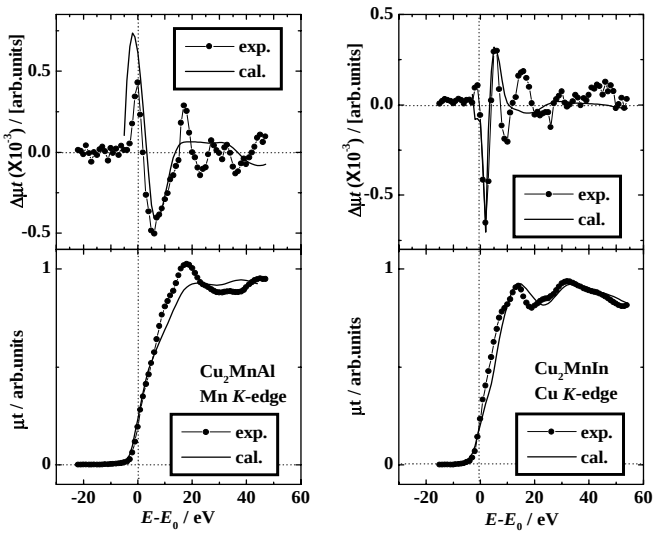

Figure 2 Comparison between the simulated and experimental XMCD (upper panel) and XANES (lower panel) spectra at the Mn *K*-edge in Cu_2MnAl (left-hand side) and the Cu *K*-edge in Cu_2MnIn (right-hand side).

simulation results of XANES and XMCD spectra at the Mn *K*-edge in Cu_2MnAl and the Cu *K*-edge in Cu_2MnIn. We only compared the *ab intio* calculation with the corresponding spectrum in Fig. 2. In the process of the simulation, we checked fitting tendency with varying the parameters.

- Charge transfer from Mn 3*d* to Cu 3*d* states
  As the charge number transferred from Mn 3*d* to Cu 3*d* is increased, the Mn *K*-edge XANES profile changes from flat peak to double peak. However, the Cu *K*-edge XANES is hardly influenced. These trends in Heusler alloy differ from those in Fe_3Al having the DO_3-type structure. In the case of Fe_3Al, the Fe *K*-edge XANES profile is broadened when charge transfer from Fe 3*d* to Al 3*p* takes place.
- Electron population
  As the electron population of Mn 3*d* orbitals is decreased, the Mn *K*-edge XANES becomes to have double peak. Even though the electron population is redistributed between Cu 3*d* and 4*s* orbitals, the Cu *K*-edge XANES maintains the original profile. On the other hand, in the case of Fe_3Al the electron redistribution between Fe 3*d* and 4*s* gave influence to the profile. This may be associated with the difference in the electronic structure; that is, Heusler alloy is classified as a typical metal, whereas Fe_3Al is composed of metallic and covalent Fe sites.
- Spin polarization
  The intensity of XMCD spectrum sensitively depends on spin polarization, while the profile and chemical shift are hardly influenced by the magnitude of spin polarization.
- Madelung potential
  In Heusler alloy, Madelung potential is indispensable for reproducing the XMCD spectrum by the FMS simulation, which means that the electron redistribution plays an important role for electronic and magnetic properties in Heusler alloy.

As shown in Fig.2, an overall agreement between the calculated and experimental spectra is fairly good. Table 1 shows the electronic structure determined for Cu_2MnAl, Cu_2MnIn and Cu_2MnSn. The difference between up- and down-spin in Mn and Cu 3*d* bands is in good agreement with the magnitude of magnetic moments in Cu_2MnAl (Felcher *et al.*, 1963).

5. Conclusions

The XANES and XMCD spectra at the Mn and Cu *K*-edge in Cu_2MnX (X=Al, In, and Sn) Heusler alloys have been recorded and analyzed by the FMS simulations. The XMCD spectral profile is very similar between the Mn and Cu *K*-edge, which indicates that Cu 4*p* polarization originates in the Mn conduction bands polarized by the 3*d*-4*p* interaction. The observed XMCD spectrum is well reproduced by the FMS calculation taking into account Madelung potential at both the Mn and Cu *K*-edge. It is concluded that charge redistribution is important factor for the electronic and magnetic states in the Cu_2MnX Heusler alloy system.

Table 1 Electron population determined from the FMS simulations.

Cu_2MnAl	Up	Down	Total	Diff.
Al 3*s*	0.65	0.64	1.29	0.01
p, d	1.37	1.39	2.75	-0.02
Mn 3*d*	4.84	0.41	5.25	4.42
s, p	0.71	0.60	1.31	0.10
Cu 3*d*	4.57	4.46	9.03	0.11
s, p	0.84	0.84	1.68	0.00
Cu_2MnIn				
In 5*s*	0.65	0.64	1.29	0.01
p, d	0.87	0.89	1.75	-0.02
Mn 3*d*	4.24	0.01	4.25	4.22
s, p	0.96	0.85	1.81	0.10
Cu 3*d*	4.94	4.83	9.78	0.11
s, p	0.84	0.84	1.68	0.00
Cu_2MnSn				
Sn 5*s*	0.90	0.89	1.79	0.01
p, d	1.12	1.14	2.25	-0.02
Mn 3*d*	4.84	1.41	6.25	3.42
s, p	0.71	0.60	1.31	0.10
Cu 3*d*	4.57	4.46	9.03	0.11
s, p	0.84	0.84	1.68	0.00

Acknowledgements

The authors express their thanks to Dr. Iwazumi of KEK-PF for his technical support and discussion. This work was carried out under the approval of KEK-PF PAC (No. 98-G024).

References

Dunlap, R.A., Stroink, G. & Dini, K. (1986). *J. Phys. F:Met. Phys.* **16**, 1083-1092

Felcher, G.P., Cable, J.W. & Wilkinson, M.K. (1963). *J. Phys. Chem. Solids* **24**, 1663-1665

Fujikawa, T. (1993). *J. Phys. Soc. Jpn* **62**, 2155-2165

Harman, F. & Skilman, S. (1963). *Atomic Structure Calculations*, (Prentic-Hall Inc. Englewood Cliffs, New Jersey)

Hatada, K. Tanaka, H. Fujikawa, T. and Hedin, L. *J. Synchrotron Rad.* (in this issue)

Ishida, S., Ishida, J., Asano, S. & Yamashita, J. (1978). *J. Phys. Soc. Jpn.* **45**, 1239-1243

Iwazumi, T., Koyama, A. & Sakurai, Y. (1995). Rev. Sci. Instrum. **66**, 1691-1693

Kawamura, N., Maruyama, H., Kobayashi, K., Uemura, S., Urata, A. & Yamazaki, H. (1999). *J. Phys. Soc. Jpn.* **68**, 923-929

Shinohara, T., (1969). *J.Phys. Soc. Jpn* **27**, 1127-1135